Yue, Zhiyuan; Cao, Zhixian; Yan, Jun

Computational Study of Flooding Due to Overtopping Breach of Landslide Dams

COMPUTATIONAL STUDY OF FLOODING DUE TO OVERTOPPING BREACH OF LANDSLIDE DAMS

Zhiyuan Yue[1], Zhixian Cao[2], Jun Yan[1]

[1] PhD candidate, State Key Laboratory of Water Resources & Hydropower Engineering Science, Wuhan University, China
[2] Corresponding author, Professor, State Key Laboratory of Water Resources and Hydropower Engineering Science, Wuhan University, Wuhan 430072, China. E-mail: zxcao@whu.edu.cn.

ABSTRACT

Breach of landslide dams may induce intense sediment transport and rapid bed evolution under high flow regime, for which traditional decoupled mathematical river models based on simplified conservation equations are not applicable. This paper presents a two-dimensional coupled mathematical river model, which is generally applicable to processes with either intense or weak sediment transport. The governing equations of the model comprise the complete shallow water hydrodynamic equations. The hyperbolic system of the governing equations is numerically solved using a second-order TVD WAF algorithm along with the HLLC approximate Riemann solver, which can properly capture shock waves and contact discontinuity for sediment transport. The computational study is corroborated with a series of laboratory experiments carried out in a laboratory flume. The computed stage hydrographs are in reasonably good agreement with the measured data collected with a set of automatic water-level probes in flume experiments, and also a modified sediment entrainment formulation. It is found that existing sediment entrainment formulations based on steady and uniform flow may not be directly applicable for breach process of landslide dams due to highly unsteady and non-uniform flows, which necessitates further studies. The flow due to breach of landslide dams is highly non-uniform such that traditional numerical schemes for gradually varied flow are not applicable, and high-resolution numerical schemes are needed. It is hard to reliably determine the discharge hydrographs at the dam-site using existing empirical relationships, which necessitates full hydrodynamic modeling of the complete domain up- and downstream of the dam.

Keywords: landslide, dam break, flooding, coupled mathematical model, sediment entrainment

1. INTRODUCTION

As an emergency disaster, flooding due to failure of landslide dams often happens around world (*e.g.* in China, in New Zealand *etc*), of which the mechanism of evolution is a topic of interest. Sediment erosion may lead to failure of landslide dams (Kuang 1993), and in this process intense sediment transport and rapid bed evolution exist under high flow regime, for which traditional decoupled mathematical river models based on simplified conservation equations are not applicable. Therefore, a coupled mathematical river model based upon complete governing equations and high-performance scheme is needed. Existing dam-break flooding models depend on empirical failure process (Oliver 2002; Zhu *et al*. 2003) and are confined to non-erodible bed case. Previous models applicable to erodible bed cases are based on a presumed dam breach finished completely and instantly (Zhang and Wang 2002; Cao *et al*. 2004; Simpson *et al*. 2006; Cao *et al*. 2007), in which the impact of gradual failure of landslide dams is considered inadequately. Faeh (2007) presents a two-dimensional decoupled mathematical model that is applied to flooding due to overtopping failure of landslide dams, however the model based on simplified equations may not describe the interaction among flow, sediment transport and bed evolution adequately.

This paper presents a two-dimensional coupled mathematical river model for flooding due to landslide dam failure. The model is built upon the shallow water hydrodynamic equations closed with Manning roughness for boundary resistance and modified empirical relationships for sediment exchange with erodible bed. A second-order TVD WAF algorithm along with the HLLC approximate Riemann solver is adopted to solve the hyperbolic system of the governing equations, which can properly capture shock waves and contact discontinuity for sediment transport. The computed stage hydrographs are in reasonably good agreement with the measured data collected with a set of automatic water-level probes in the flume experiments.

2. MATHEMATICAL FORMULATIONS

2.1 Governing equations

The governing equations of the 2D shallow water hydrodynamic model comprise the complete mass and momentum conservation equations for the water-sediment mixture flow and the mass conservation equations respectively for sediment and bed material. The equations can be derived from the fundamental conservation laws in fluid dynamics (Batchelor 1967), which constitute a fifth-order hyperbolic system for five unknowns (flow depth, two velocity components, sediment concentration and bed elevation). With a simple form, the equation describing bed deformation is separated from the remaining four equations in order to expedite mathematical manipulation. The equations of flow and sediment transport are rewritten as,

$$\frac{\partial \mathbf{U}}{\partial t}+\frac{\partial \mathbf{F}}{\partial x}+\frac{\partial \mathbf{G}}{\partial y}=\mathbf{S} \tag{1}$$

$$\mathbf{U}=\begin{bmatrix} h \\ hu \\ hv \\ hc \end{bmatrix}, \quad \mathbf{F}=\begin{bmatrix} hu \\ hu^2+gh^2/2 \\ huv \\ huc \end{bmatrix}, \quad \mathbf{G}=\begin{bmatrix} hv \\ huv \\ hv^2+gh^2/2 \\ hvc \end{bmatrix}, \tag{2a, b, c}$$

$$\mathbf{S}=\begin{bmatrix} (E-D)/(1-p) \\ gh(S_{bx}-S_{fx})+\varepsilon\left(\dfrac{\partial^2 hu}{\partial x^2}+\dfrac{\partial^2 hu}{\partial y^2}\right)-\dfrac{(\rho_s-\rho_w)gh^2}{2\rho}\dfrac{\partial c}{\partial x}-\dfrac{(\rho-\rho_0)(E-D)u}{\rho(1-p)} \\ gh(S_{by}-S_{fy})+\varepsilon\left(\dfrac{\partial^2 hv}{\partial x^2}+\dfrac{\partial^2 hv}{\partial y^2}\right)-\dfrac{(\rho_s-\rho_w)gh^2}{2\rho}\dfrac{\partial c}{\partial y}-\dfrac{(\rho-\rho_0)(E-D)v}{\rho(1-p)} \\ E-D \end{bmatrix} \tag{2d}$$

$$\frac{\partial z}{\partial t} = \frac{D - E}{1 - p} \tag{3}$$

where $\mathbf{U}$ = vector of conserved variables; $\mathbf{F}, \mathbf{G}$ = vectors of flux variables; $\mathbf{S}$ = vector of source terms; t = time; x, y = horizontal coordinates; h = flow depth; u, v = depth-averaged velocities in the x- and y-directions; z = bed elevation; c = averaged sediment concentration in volume; g = gravitational acceleration; S_x, S_y = friction slope in x- and y-directions; p = bed sediment porosity; E, D = sediment entrainment and deposition fluxes across the bottom boundary of the flow; ρ_w, ρ_s = densities of water and sediment; $\rho = \rho_w(1-c) + \rho_s c$ = density of water-sediment mixture; $\rho_0 = \rho_w p + \rho_s(1-p)$ = density of saturated bed; and S_{bx}, S_{by} = bed slope in x- and y-directions, respectively; ε = coefficient of turbulent viscosity.

2.2 Empirical closure relationships

The friction slope is determined by the conventional relationship, which involves the Manning roughness n,

$$S_x = \frac{n^2 u\sqrt{u^2+v^2}}{h^{4/3}}, \qquad S_y = \frac{n^2 v\sqrt{u^2+v^2}}{h^{4/3}} \tag{4}$$

Sediment deposition flux is calculated by

$$D = w(1-c_a)^m c_a \tag{5}$$

where D = near-bed sediment concentration in volume, which is related to the averaged sediment concentration by $c_a = \alpha c$, where α = min(2, (1-p)/c); w = settling velocity of a single sediment particle in tranquil water; the exponent m = $4.45R^{-0.1}$, where d = particle diameter, $R \equiv \sqrt{sgd}\, d/\nu$, ν = kinematic viscosity of water, and $s = \rho_s/\rho_w - 1$.

There have been a plethora of empirical relationships for sediment entrainment, which are essential for closing the mathematical model. In the present investigation three empirical formulas have been adopted respectively,

Zyserman and Fredsoe (1994) (ZF)

$$E = \begin{cases} w(1-c_e)^m c_e & \theta \ge \theta_c \\ 0 & \theta < \theta \end{cases}, \quad c_e = \frac{0.15226(\theta-\theta_c)^{1.75}}{0.46 + 0.331(\theta-\theta_c)^{1.75}} \tag{6a, b}$$

Cao *et al*. (1999) (CAO)

$$E = \begin{cases} \dfrac{560}{3R^{0.8}} \dfrac{(1-p)}{\theta_c} \dfrac{(\theta-\theta_c)d}{h}\sqrt{u^2+v^2}, & \theta \ge \theta_c \\ 0 & \theta < \theta \end{cases} \tag{6c, d}$$

Garcia and Parker (1991) (GP)

$$E=\begin{cases}\dfrac{A}{1+\dfrac{A}{0.3}Z_u^5}\,, & \theta\ge\theta_c \\ 0 & \theta<\theta\end{cases}\,,\quad Z_u=\frac{u_*}{\nu}R^{0.6}\,,\ \mathrm{A}=1.3\times10^{-7} \qquad \text{(6e, f)}$$

where $\theta = u_*^2 / sgd$ = Shields parameter; θ_c = critical Shields parameter; u_* = bed shear velocity.

2.3 Numerical scheme

The second-order Total-Variation-Diminishing version of the Weighted-Average-Flux method, along with the HLLC approximate Riemann Solver, is adapted to solve the governing equations, which can properly resolve shock waves and contact discontinuities. This is essentially a slightly adapted version of the more general numerical algorithm reported in Cao *et al*. (2007).

3. NUMENRICAL MODELING OF LADSLIDE DAM FAILUE

A series of experiments of flooding due to landslide dam failure have been accomplished in a large-scale flume (Yan *et al*. 2006). The stage hydrographs at ten cross sections measured with a set of automatic stage metes provide unique datasets for the test of the present mathematical model.

3.1 Numerical modeling approach

The initial condition represents an essentially steady and non-uniform flow along the channel, as illustrated by free surface profile in Figure 1 before a landslide dam is formed. Following the landslide, water waves are triggered, and yet the waves are not directly taken into account in the numerical modeling as the waves are limited to the very early stage of the entire process. With this approximation, the initial state in the numerical modeling actually corresponds to the scenario shown in Figure 2, with the landslide dam already in place. Also, the effects of infiltration through the landslide dam are estimated to be very limited due to the fine sediment particle sizes and thus neglected in the numerical modeling. The upstream boundary is prescribed by the inlet discharge, while at the outlet of the channel the stage hydrograph measured is imposed as downstream boundary condition.

3.2 Numerical study of flooding due to landslide dam failure

Figure 3 shows the stage hydrographs by the flume experiments and numerical model with direct application of the three empirical relationships for sediment entrainment [Eq. (6a-f)]. Obvious deviations of the numerical results from the experimental data can be seen, which indicates that existing sediment entrainment formulations derived under steady and uniform flows cannot describe sediment transport under high flow regime.

An attempt is made to reconcile the numerical modeling hydrographs with the experimental data by modifying the ZF sediment entrainment formula, as follows,

$$E^* = \varphi E \tag{7a}$$

where $E^* =$ modified entrainment formula ; $E =$ ZF empirical relationship for entrainment flux by Eq. (6a, b), and $\varphi =$ correctional coefficient, which is given by

$$\varphi = \begin{cases} 0.2 & t \le t_0 \\ 1 & t_0 \le t \le t_0 + t_1 / 2 \\ 0.8 & t_0 + t_1 / 2 \le t \le t_0 + t_1 \\ 0.1 & t \ge t_0 + t_1 \end{cases} \tag{7b}$$

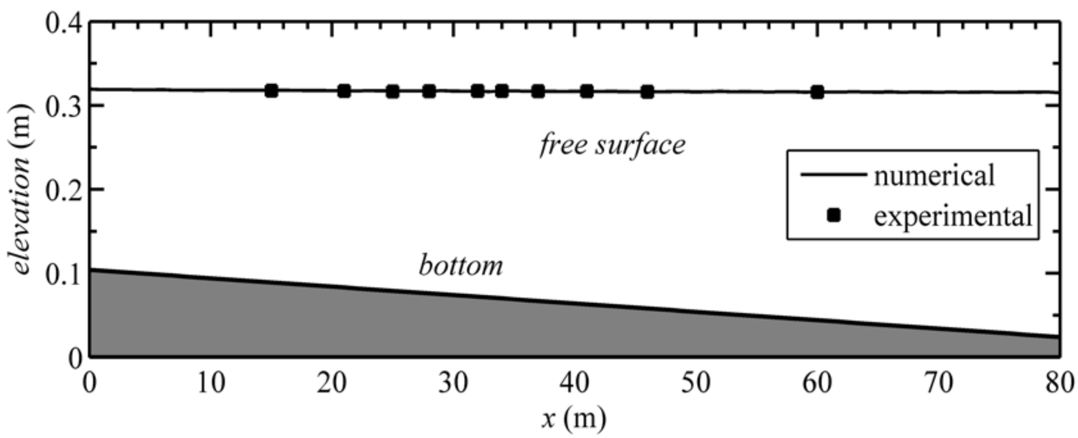

Figure 1. Comparison between computed and experimental free surface level

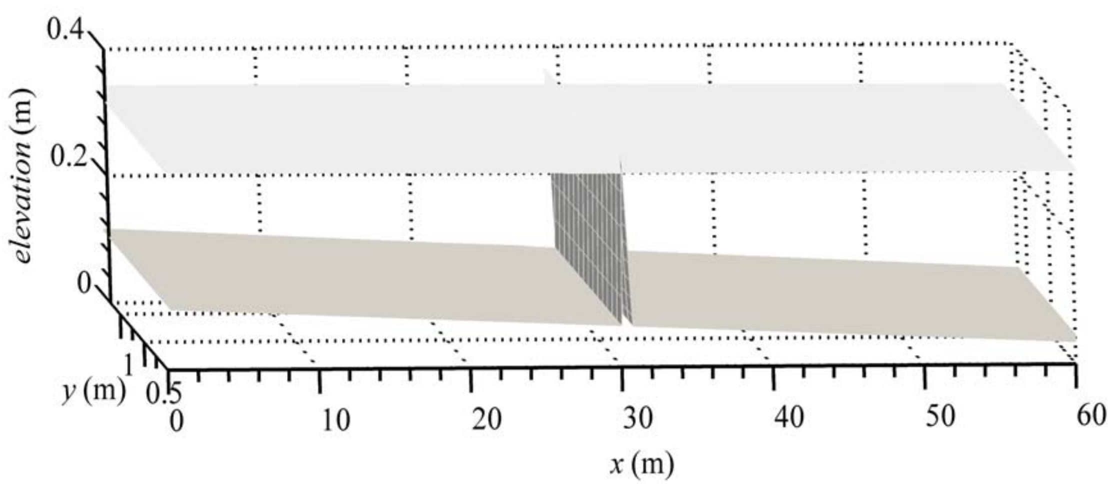

Figure 2. Initial free surface and bed elevation

Figure 4 shows the stage hydrographs by the experiments and the numerical model with the modified sediment entrainment function Eq. (7). Reasonably good agreement between the numerical results and measurements is obtained, which is encouraging. However, slight discrepancies between them can be identified due to following factors: (a) the effects of the initial waves and infiltration are not considered; (b) the failure process of landslide dams involve complicated flow-earth interactions, of which the mechanism remains poorly understood and its quantification rather uncertain. Eq. (7) represents a tentative correction to one of the sediment entrainment functions derived for steady and uniform flows. Further investigation is apparently critical for refined modeling of landslide dam break flooding.

Figure 5 shows elevation of stage and bed at the site of landslide dams. It is seen that stage and bed elevation undulates in *x*-direction, which indicates that failure of landslide dam may induce strong non-steady flow or shock waves. Obviously, the flow due to breach of landslide dams is highly non-uniform and even feature shock waves such that traditional numerical schemes for gradually varied flows are not applicable, and high-resolution numerical schemes are necessary.

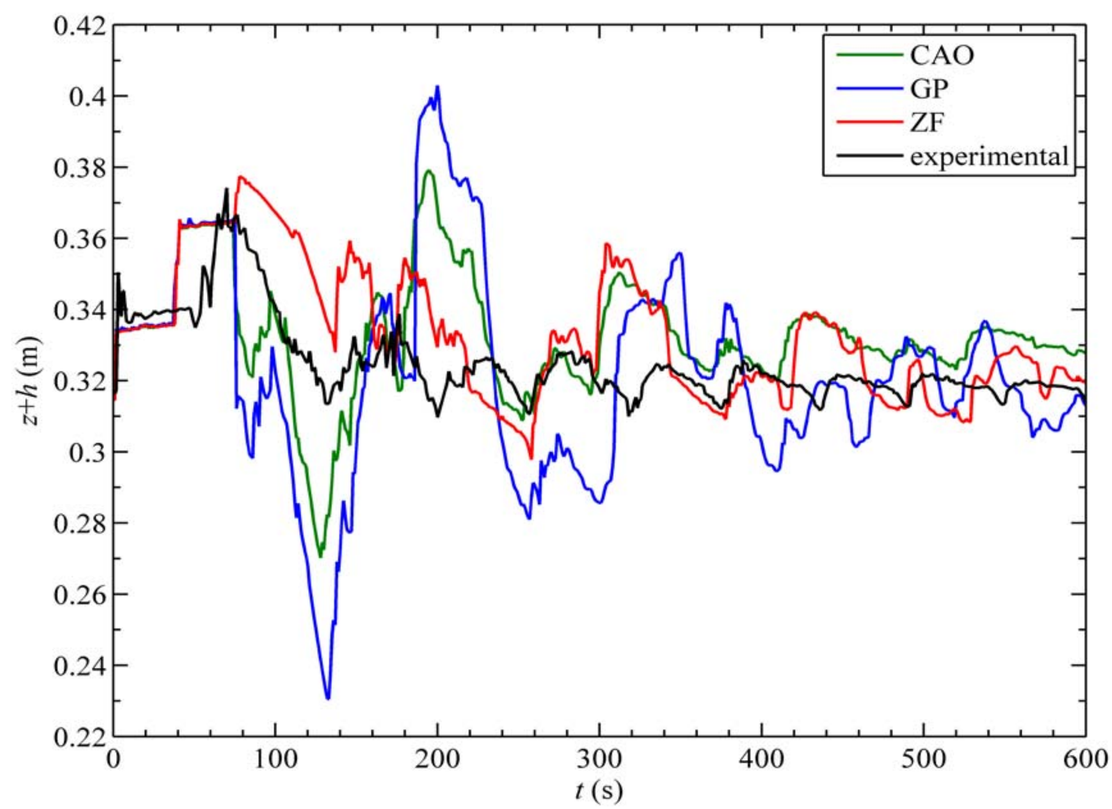

Figure 3. Stage hydrographs for the experiments and numerical model with three empirical relationships for sediment entrainment

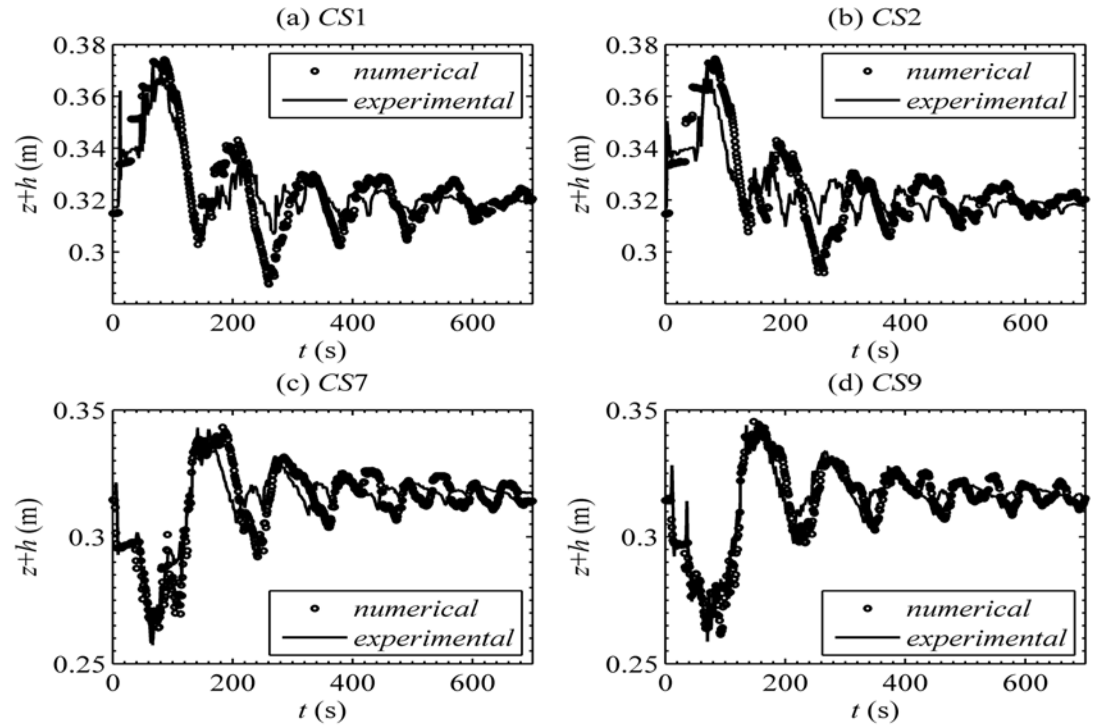

Figure 4. Stage hydrographs for the experimental data and numerical results with modified empirical relationship for sediment entrainment

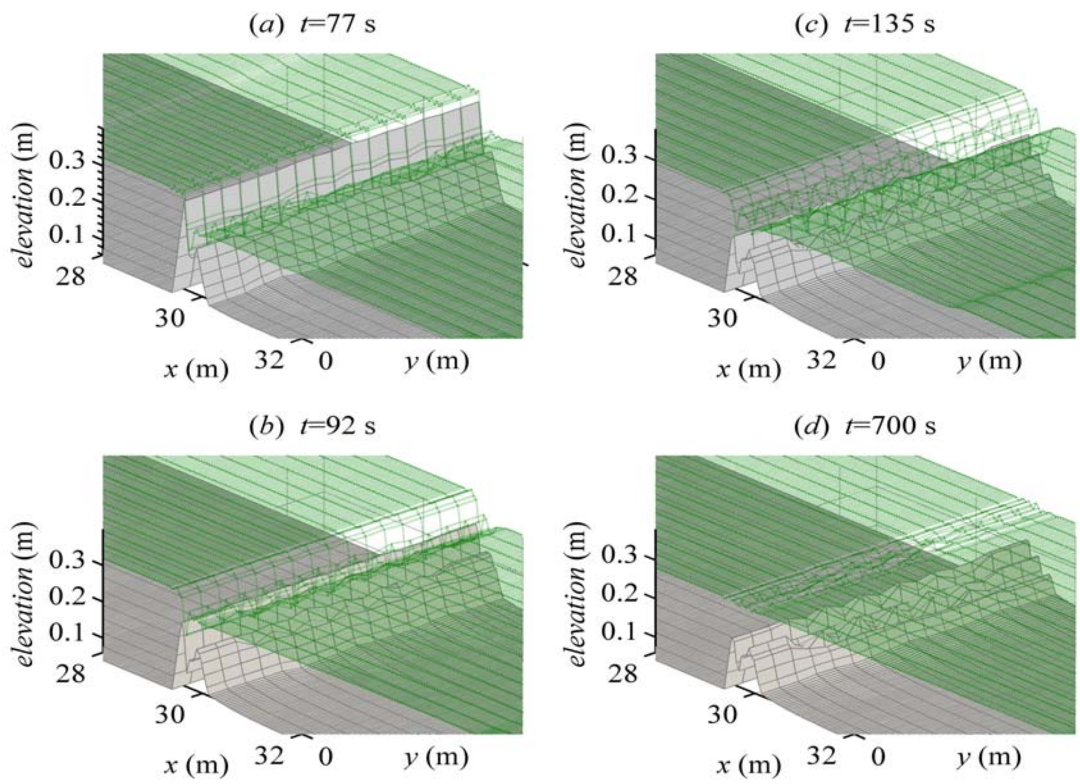

Figure 5. Elevation of stage and bed at the site of the landslide dams

There have been a number of empirical relationships for estimating the discharge hydrographs of flood due to dam-break, which involve the basic parameters of the reservoirs and the breach openings.

Chanson (2005, referred to as CH)

$$Q_b = \frac{2}{3} C_D \sqrt{\frac{2}{3} g E_1{}^3} B_{\max} \tag{8-a}$$

$$\frac{z_{lip}}{d_0} = 1.08 e^{\left(-0.0013 t \sqrt{\frac{g}{d_0}}\right)}, \qquad \text{for } 60 < t\sqrt{\frac{g}{d_0}} < 1750 \tag{8-b}$$

$$\frac{B_{\max}}{d_0} = 2.73 \times 10^{-4\left(t\sqrt{\frac{g}{d_0}}\right)^{1.4}}, \qquad \text{for } t\sqrt{\frac{g}{d_0}} < 1000 \tag{8-c}$$

$$\frac{B_{\min}}{d_0} = 4.01 \times 10^{-7\left(t\sqrt{\frac{g}{d_0}}\right)^{2.28}}, \qquad \text{for } t\sqrt{\frac{g}{d_0}} < 1000 \tag{8-d}$$

Walder and O'Connor (1997, referred to as WO)

WO1: $$Q_p = 1.6 V_0^{0.46} \tag{9-a}$$

WO2: $$Q_p = 6.7 d_H{}^{1.73} \tag{9-b}$$

WO3: $$Q_p = 0.99 (d_H V_0)^{0.4} \tag{9-c}$$

where E_1 = upstream specific energy above centerline dam breach elevation; Q_b = discharge at dam site; $B_{\max}$ = free surface width at the upper lip of the breach; e = 2.718; C_d = 0.6 $m^{1/2}/s$; $z_{\min}$ = inlet lip elevation on the breach centreline; d_0 = reservoir height; $B_{\min}$ = free surface width at the breach throat; Q_p = peak discharge; d_H = fall for free surface level in front of landslide dam; V_0 = water volume in front of landslide dams.

In contrast to the empirical relationships, the discharge hydrographs at the dam-site can be directly obtained as a result of the present hydrodynamic model. Figure 6 shows a comparison between the discharge hydrographs at the dam-site from the present numerical model and Chanson's (2005) method, and Table 1 shows a comparison between the peak discharges at the site of dam-site from the present numerical model and a selection of existing of empirical methods [Eqs. (8) and (9)]. It is seen that the full discharge hydrograph cannot be reproduced by Chanson's (2005) method (Figure 6), and the differences between the empirical and numerical modeling peak discharges (Table 1) are considerable. It is noted that traditional dam-break flood models resolve flood propagation in the downstream using the discharge hydrographs estimated using existing empirical relationships as boundary conditions, in contrast to the present model that resolves the discharge as part of the solution. Therefore traditional models for dam-break floods are insufficient and need to be reformulated.

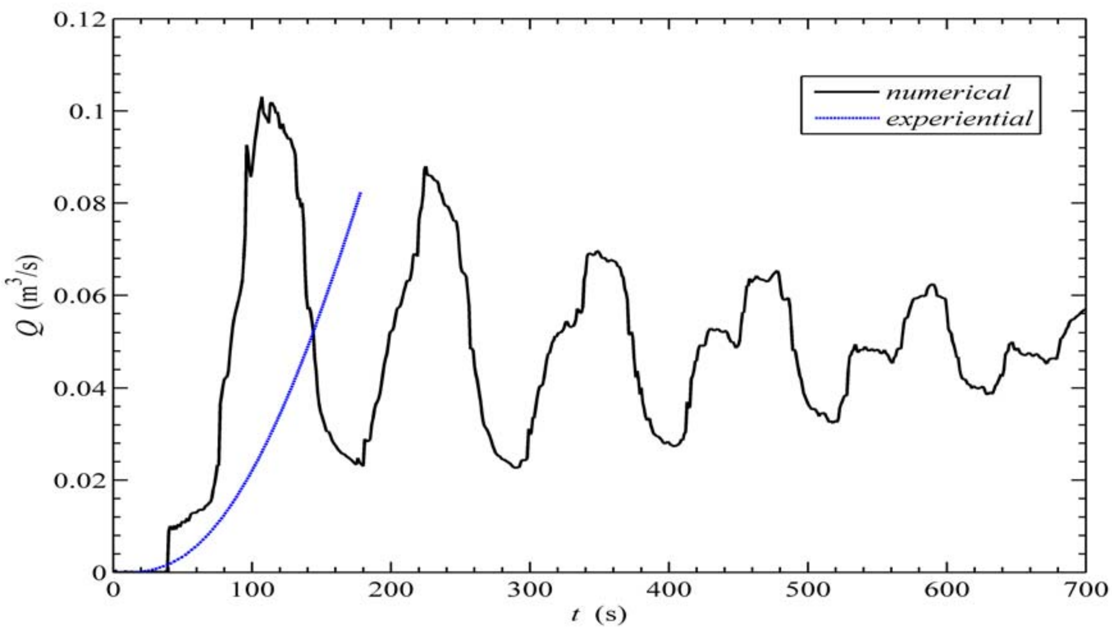

Figure 6. Comparison between discharge hydrographs at dam-site by numerical model and Chanson's (2005) method

Table 1. Comparison between peak discharges at site of landslide dam by numerical model and empirical methods

Methods	Present model	CH	WO1	WO2	WO3
Peak discharge (m^3/s)	0.103	0.08	4.19	0.1	0.87

4. CONCLUSION

Flooding due to landslide dam failure is studied from a 2D coupled flow-sediment mathematical model. The theoretical model is built upon the complete shallow water hydrodynamic equations closed with Manning roughness for boundary resistance and slightly modified empirical relationships for sediment exchange with erodible bed and the second-order Total-Variation-Diminishing version of the Weighted-Average-Flux method, along with the HLLC approximate Riemann Solver, is adapted to solve the governing equations, which can properly resolve shock waves and contact discontinuities. The model is applied to the pilot study of the flooding due to overtopping failure of landslide dams and the experimental data is employed to examine the validity of the present model. Good agreement between numerical results and measurements is found. Existing sediment entrainment formulations based on steady and uniform flow seem to not be directly applicable for the breach process of landslide dams due to highly unsteady and non-uniform flows, which necessitates the further study. Meanwhile, traditional numerical schemes for gradual varied flow are not applicable for shock waves, which may occur during the breach of landslide dams, thus high-performance numerical schemes are needed. Moreover, traditional mathematical models for dam-break floods need to be reformulated since it is hard to appropriately estimate the discharge hydrograph at the dam-site using existing empirical relationships.

ACKNOWLEDGMENTS

This investigation is funded by the National Key Basic Research and Development Program (973 program) of China (Grant No. 2007CB714106).

REFERENCES

Batchelor, G. (1967), An Introduction to Fluid Dynamics, Cambridge University Press, England.

Billett, S., and Toro, E. (1997), On WAF-type schemes for multidimensional hyperbolic conservation laws, *Journal of Computational Physics*, 130, 1-24.

Cao, Z. (1999), Equilibrium near-bed concentration of suspended sediment, *Journal of Hydraulic Engineering*, ASCE, 125(12), 1270-1278.

Cao, Z., Pender, G., Wallis, S., and Carling, P. (2004), Computational dam-break hydraulics over erodible sediment bed, *Journal of Hydraulic Engineering*, ASCE, 130, 689-703.

Cao, Z., Yue, Z., Li, X., and Che, T. (2007), Two-dimensional mathematical modeling of flooding over erodible sediment bed, *Proc. 32nd IAHR Congress*, July, Venice, Italy.

Chanson, H. (2005), The 1786 earthquake-triggered landslide dam and subsequent dam-break flood on the Dadu River, southwestern China, *Journal of Hydrology*, Elsevier, 71(3-4), 437-440.

Faeh, R. (2007), Numerical Modeling of Breach Erosion of River Embankments, *Journal of Hydraulic Engineering*, ASCE, 133(9), 1000-1009.

Garcia, M. and Parker, G. (1991), Entrainment of bed sediment into suspension, *Journal of Hydraulic Engineering*, ASCE, 117(4), 1414-435.

Hubbard, M. and Dodd, N. (2002), A 2D numerical model of wave run-up and overtopping, *Coastal Engineering*, 47, 1-26.

Kuang, S. (1993), Formation Mechanisms and Prediction Models of Debris Flow due to Natural Dam Failures, *Journal of Sediment Research*, 4, 42-57.

Oliver, K. (2002), Recent research on landslide dams - a literature review with special attention to New Zealand, *Progress in Physical Geography*, 26, 206-235.

Simpson, G. and Castelltortb, S. (2006), Coupled model of surface water flow, sediment transport and morphological evolution, Computers & Geosciences, 32, 1600-1614.

Sleigh, P., Gaskell P., Berzins, M., and Wright, N. (1998), An unstructured finite-volume algorithm for predicting flow in rivers and estuaries, *Computers and Fluids*, 27, 479-508.

Toro, E. (2001), Shock-Capturing methods for free-surface shallow flows, Wiley, England.

Walder, J. and O'Connor, J. (1997), Methods for predicting peak discharge of floods caused by failure of natural and constructed earthen dams, *Water Resources Research*, 33(10), 2337-2348.

Yan, J., Cao, Z., and Chen, L. (2006), Experimental study of landslide-induced flooding in open channels, *International Conference on Fluvial Hydraulics*: River Flow, Lisbon, Portugal.

Zhang, X. and Wang, G. (2002), Flow analysis and scour computation of the dike-break, *Journal of Sediment Research*, 1, 18-24.

Zhu, Y., Liao, H., and Wu, Z. (2003), The earth-dam-break model and its development, *Journal of Hydroelectric Engineering*, 81, 31-38.

Zyserman, B. and Fredsoe, J. (1994), Data analysis of bed concentration of suspended sediment, *Journal of Hydraulic Engineering*, ASCE, 120(9), 1021-1042.